*Journal of Nano- and Electronic Physics*
Vol. **15** No 5, 05032(7pp) (2023)

*Журнал нано- та електронної фізики*
Том **15** № 5, 05032(7cc) (2023)

# MHD Natural Convection of $Fe_3O_4$-Water Nanofluid in a Cubic Cavity

M. Maache Battira[1,*], C. Brahmi[1], R. Bessaih[2]

[1] *Abbes Laghrour University, Faculty of Science and Technology, Department of Mechanical Engineering, 40000 Khenchela, Algeria*
[2] *Mentouri University, Faculty of Science and Technology, Department of Mechanical Engineering, 25000 Constantine, Algeria*

(Received 26 July 2023; revised manuscript received 18 October 2023; published online 30 October 2023)

The effect of the three main directions of a uniform external magnetic field on the free convection in a cubic cavity differentially heated and filled with the $Fe_3O_4$-$H_2O$ nanofluid is numerically studied. The finite volume method is chosen for the discretization of the system of partial differential equations governing the MHD phenomenon and the numerical resolution is made using the Ansys-Fluent 14.5 software. In this work, the problem was studied for pure water ($\emptyset = 0$), then for water with the addition of small proportions of nanoparticles ($\emptyset = 1\%, 2\%, 3\%$ and $4\%$). The effect of the three main magnetic field directions, the Hartmann number ($Ha = 0, 5, 10, 15$ and $20$) and the Rayleigh number ($Ra = 10^3,\ 10^4,\ 10^5$ and $10^6$), on the thermo-hydrodynamic nanofluid behavior is examined. The thermal conductivity and the dynamic viscosity are determined by correlations specifically elaborated for $Fe_3O_4$-$H_2O$ nanofluid from anterior experimental works. Results of this numerical simulation show that, the more the value of Rayleigh number increases, the more the slope of the decrease of the Nusselt number with the increase of the intensity of the magnetic field becomes stronger. The horizontal application of the magnetic field, i.e. parallel to the temperature gradient, reduces the heat transfer more than the other two directions. In the second position, the greatest decrease in the rate of convective heat transfer is recorded when the direction of the magnetic field is vertical, i.e. in the direction of gravity.

**Keywords:** Cubic cavity, Natural convection, Magnetic field direction, $Fe_3O_4$-$H_2O$ nanofluid.

DOI: 10.21272/jnep.15(5).05032 PACS numbers: 44.25. + f, 47.11.Df

## 1. INTRODUCTION

Impacts of the external magnetic field (MF) on natural convection thermal transfer in square enclosures filled with nanofluids (nnfs) have been the subject of much scientific research for the last two decades [1]. This phenomenon called magnetohydrodynamics (MHD) can be encountered in many industrial fields, like heat exchangers, solar technology, electronic and microelectronic devices, etc. Due to the significant thermal conductivity of nanoparticles (nnps), the thermal conductivity of nnfs is higher than that of base fluids [2]. In many cases, the free convective thermal exchange efficiency can be dramatically enhanced by employ nnfs as the working medium. It is also easily controlled by the application of MF which leads to a reduction in convective currents. The study further reveals that the use of Cu nnps promotes heat exchange more than the use of $TiO_2$ or $Al_2O_3$. M. Hajiyan et al. [3] study numerically the effect of applying an external uniform MF on free convection of a magnetic nnf into a square cavity. They consider the relation between thermal conductivity of magnetic nnf at different nnps concentrations and the MF intensity. They use the Brinkman model for predicting dynamic viscosity and for thermal conductivity, six models from literature models are used. They find that as Ra increases the Nu increases. In contrast, convective heat transfer declines when the intensity of MF decreases because of suppressing the buoyancy force by the strong MF. Z. Boulahia et al. [4] present a numerical irreversibility analysis of two-dimensional and three-dimensional naturel convection MHD within cubic cavity filled with hybrid nnf (alumina, copper and titanium dioxide with water as base fluid). They use Corcione correlations for dynamic viscosity and thermal conductivity of hybrid nanofluid. This study shows that varying Ha, Ra and the MF angle, the thermal transfer rate and entropy creation are visibly changed. In addition, it is demonstrated that to have a satisfactory enhancement heat exchange rate, the effect of rising the concentration of hybrid nnps can be optimized. L. El Moutaouakil et al. [5] analyze numerically the impact of the orientation of three heating elements on the free convection of nnfs in a partially heated cubic enclosure with considering thermal radiation. Several nanofluids ($Al_2O_3$, Cu, $TiO_2$, Ag) with water-based fluid are used. Classical models for predicting thermal conductivity and dynamic viscosity (Maxwell and Brinkman) are used. Results demonstrate that the inclination angle has a significantly influences the thermal and dynamic fields, but its influence on the thermal transfer is inconsiderable. The Nu enhances with Ra, the radiation parameter, the nnps volume fraction and the heated elements aspect ratio. M. Ferhi et al. [6] use a Lattice Boltzmann Method to study the free conjugate thermal exchange and entropy generation in MWCNT-water nnf in a partially heated divided enclosure. The outcomes show the MF direction have a significant impact on the heat exchange rate and the rise in MF intensity decreases the heat exchange and the heat generation in the enclosure.

It emerges from the extensive bibliographical research that most scientific works carried out have adopted some well-known nnps such as $Al_2O_3$, $TiO_2$,

* mounamaache@yahoo.fr

 

CuO, etc. [7]. The precision of the models for calculating the effective dynamic viscosity and thermal conductivity of these common nnfs represents a serious problem in using these substances especially in numerical studies. While, many researchers show that the use of specific models can conduct to inaccurate values of these thermophysical properties [8]. D. Toghraie et al. [9] determine the $Fe_3O_4$-water nnf dynamic viscosity experimentally. The experiments were carried out for limited temperature values between 20 °C and 55 °C with low nnps volume fraction ($\emptyset \leq 3\%$). The results show that the viscosity reduces significantly with growing temperature. Also, the viscosity increases extensively with the rising of nnps concentration. For this work, the model of dynamic viscosity found experimentally by D. Toghraie et al. [9] is adopted. M. Afrand et al. [10] developed a correlation to evaluate the thermal conductivity of $Fe_3O_4$-water nnf. They succeed in expressing the variation of the nnf thermal conductivity depending on the nnps volume fraction and the temperature. Their correlation for predicting the $Fe_3O_4$-water thermal conductivity is adopted for this study.

The main goal of this 3D numerical investigation is to highlight the thermal transfer behavior of a cubic enclosure when a low solid volume fraction of $Fe_3O_4$ is seeded in water inside it. The enclosure is exposed externally to a uniform MF, directed, in one of the principal directions *x*, *y* or *z*. Simulations are performed to determine the relationship between the behavior of heat exchange with varying the intensity and direction of the MF. The models adopted for estimate thermal conductivity and effective dynamic viscosity are correlations experimentally found especially for nnf with small concentrations of $Fe_3O_4$ nnps in water. To the best authors' knowledge, these two correlations have never been used together in previous studies. In addition, the use of $Fe_3O_4$-water nnf with low solid volume fraction to maintain the Newtonian character in MHD problems, is still rare in previous studies.

## 2. PROBLEM STATEMENT

### 2.1 Geometry Description

Fig. 1 shows a schema of a cubical cavity of side *L*. The $Fe_3O_4$-water nanofluid is enclosed in the cavity and subjected to differentially horizontal temperatures resulting in the free convective flow of the nnf.

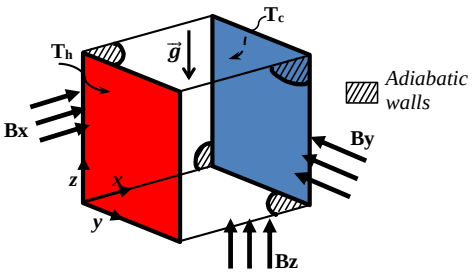


**Fig. 1** – The studied configuration

The left side wall is kept at high-temperature $T_h$ and the right-side wall is maintained at low-temperature $T_c$, while the remaining four walls are supposed to be insulators. The direction of the externally applied MF is changed in the three main directions. The strength of the MF changes. The system (*x, y, z*) is adopted. The gravity direction is the negative *z*-axis, and the temperature gradient is imposed in the x-direction. Thermo-physical properties of pure water considered as base fluid, and the magnetite nnps are presented in Table 1.

**Table 1** – Thermo-physical properties of water and $Fe_3O_4$ nanoparticles [11]

| | Pure water | $Fe_3O_4$ |
|---|---|---|
| $\rho$ [kg/m$^3$] | 997.1 | 5200 |
| $\beta$ [$10^{-5}$K$^{-1}$] | 21 | 670 |
| $k$ [W · m$^{-1}$K$^{-1}$ | 0.613 | 6 |
| $c_p$ [J · kg$^{-1}$K$^{-1}$] | 4179 | 20.796 |
| $\sigma$ [$\Omega^{-1}$m$^{-1}$] | 0.05 | 25000 |

### 2.2 Governing Equations

The flow regime is assumed to be steady and laminar. The nnf resulting from the mixture of water and magnetite ($Fe_3O_4$) is incompressible and thermally balanced, so the single-phase model is employed. The $Fe_3O_4$-Water nnf is Newtonian; it is important to explain that the Newtonian nnf hypothesis used for this simulation is valid. Since the base fluid used is the water which is a Newtonian fluid, and the solid volume fraction considered is relatively low ($\emptyset \leq 0.04$), the behavior of the nnf (particularly in terms of viscosity) is therefore similar to that of the base fluid. The Boussinesq approximation is adopted in this study, so all thermodynamic properties of nnf are assumed constant, and the variation of density is negligible in all terms of conservation equations except in the term of buoyancy forces. The Joule effect, radiation heat transfer, induced MF and viscous dissipation are neglected.

The MF vector is written as: $\vec{B} = B_0\,\vec{e_B}$. ($\vec{e_B}$: unit vector). In the case where the MF is applied in x direction: $\vec{B} = \vec{B_x} = B_0\,\vec{\imath}$. When the MF direction is *z*: $\vec{B} = \vec{B_z} = B_0\,\vec{k}$. If the MF is applied in y direction: $\vec{B} = \vec{B_y} = B_0\,\vec{\jmath}$. The electromagnetic force $\vec{F}$ is expressed by $\vec{F} = \vec{J} \times \vec{B}$ where $\vec{J}$ is the electric current. $\vec{J} = \sigma\left[-\nabla\Phi + \left(\vec{V} \times \vec{B}\right)\right]$. By using $L$, $\alpha_f/L$, $(T_h - T_c)$ and $\rho_{nf}\,\alpha_f^2/L^2$ as typical scales for lengths, velocities, temperature and pressure, respectively, the dimensionless governing equations are written by:

$$\nabla.\vec{V} = 0, \tag{1}$$

$$\left(\vec{V}.\nabla\right)\vec{V} = -\nabla P + \frac{\mu_{nf}}{\alpha_{nf}\rho_{nf}}\nabla^2\vec{V} - \frac{\rho_f\,\beta_{nf}}{\rho_{nf}\beta_f}\,Ra\,\mathrm{Pr}\,T\,\vec{k} + \\ + \frac{\sigma_{nf}\,\rho_f}{\sigma_f\,\rho_{nf}}Ha^2\,Pr\left[\left(\vec{V} \times \vec{e_B}\right) \times \vec{e_B}\right], \tag{2}$$

$$\vec{V}.\nabla\theta = \frac{\alpha_{nf}}{\alpha_f}\,\nabla^2\theta. \tag{3}$$

Dimensionless numbers are:
Rayleigh number:

$$Ra = \frac{g\,\beta_f\,(T_h - T_c)\,L^3}{\nu_f\;\alpha_f}. \tag{4}$$

Hartmann number:

$$Ha = B_0\, L \sqrt{\frac{\sigma_{nf}}{\rho_{nf}\mu_f}}. \quad (5)$$

Prandtl number:

$$Pr = \frac{\nu_f}{\alpha_f}. \quad (6)$$

The effective density, specific heat and thermal expansion coefficient of nnf are expressed as [12, 13]:

$$\rho_{nf} = \emptyset\, \rho_s + (1-\emptyset)\, \rho_f, \quad (7)$$

$$(\rho\, c_p)_{nf} = \emptyset\, (\rho\, c_p)_s + (1-\emptyset)\, (\rho\, c_p)_f, \quad (8)$$

$$(\rho\, \beta)_{nf} = \emptyset\, (\rho\, \beta)_s + (1-\emptyset)\, (\rho\, \beta)_f. \quad (9)$$

Where $\emptyset$ is the $Fe_3O_4$ volume fraction.

The effective electrical conductivity of nnf developed by Maxwell [14]:

$$\sigma_{nf} = \sigma_f \left[1 + \frac{3\,\emptyset\,(\sigma_s/\sigma_f - 1)}{(\sigma_s/\sigma_f + 2) - \emptyset(\sigma_s/\sigma_f - 1)}\right]. \quad (10)$$

For small solid volume fractions of $Fe_3O_4$-water, correlations are experimentally developed to estimate the thermal conductivity [10] and the dynamic viscosity [9]. These correlations are chosen to modelling these physical properties respectively:

$$\mu_{nf} = \mu_f (1.01 + 0.007165\, T^{1.171} \emptyset^{1.509}) \times \exp(-0.00719\, T)\,, \quad (11)$$

$$k_{nf} = k_f (0.7575 + 0.3\, \emptyset^{0.323} T^{0.245}), \quad (12)$$

where $\phi$ is in % and $T$ is in °C.

### 2.3 Boundary Conditions

At the right wall $T = T_c$, at the left wall $T = T_h$, and for the other four walls $\partial T/\partial n = 0$ are the thermal boundary conditions adopted for this problem.

On the left hot wall:

$$X = 0 \qquad U = V = W = 0; \qquad \theta = 1. \quad (13\text{-a})$$

On the right cold wall:

$$X = 1 \qquad U = V = W = 0; \qquad \theta = 0. \quad (13\text{-b})$$

On the four adiabatic walls:

$$Y = 0,\ Y = 1,\ Z = 0,\ Z = 1$$
$$U = V = W = 0;\ \partial\theta/\partial n = 0. \quad (13\text{-c})$$

For the electrical potential, boundary condition considered on all walls is $\partial\Phi/\partial n = 0$. For current density on all walls, the boundary condition is $\vec{J} \cdot \vec{n} = 0$.

### 2.4 Nusselt Number

At the left wall with high temperature $T_c$, the local Nu is calculated by:

$$Nu = -\frac{k_{nf}}{k_f} \left.\frac{\partial\theta}{\partial X}\right|_{X=0}, \quad (14)$$

and the average Nu is defined by:

$$Nu_{avg} = \int_0^1 \int_0^1 Nu\, dY\, dZ. \quad (15)$$

## 3. NUMERICAL SOLUTION

The simulations are made through ANSYS fluent 14.5, based on the finite volume method developed by Patankar [15]. For coupling the velocity field and pressure, the SIMPLE algorithm is used, and for pressure discretization a PRESTO scheme is applied. The 2-order upwind-scheme is chosen for discretizing the convection-diffusion terms.

### 3.1 Grid Independency

A test of sensibility of five mesh sizes is conducted as shown in Table 2. The $Nu_{avg}$ is calculated for natural convection of $Fe_3O_4$-water nnf when $Ra = 10^4$, $\phi = 0.01$, $Ha = 10$ with MF applied in temperature gradient direction ($B_x$). The code convergence test for this simulation is: $max|\Gamma^{n+1} - \Gamma^n| < 10^{-6}$ where $\Gamma$ replaces the unknown variables ($U$, $V$, $W$, $\theta$) describing the thermos-hydrodynamic behavior in the cavity and n is the number of iterations. A grid size of $71^3$ is chosen because it ensures the grid independent solution and agrees with the precision and the calculation time.

**Table 2** – Mesh analysis for, $Ra = 10^4$, $\phi = 0.01$, $Ha = 10$ (Bx)

| Mesh size | $41^3$ | $51^3$ | $61^3$ | $71^3$ | $81^3$ |
|---|---|---|---|---|---|
| $Nu_{avg}$ | 1.9998 | 1.9452 | 1.9261 | 1.9266 | 1.9267 |

### 3.2 Validation

The code used in this simulation is validated by the results obtained by Ghasemi et al. [16] on $Al_2O_3$-water in a square enclosure. Fig. 2 shows the dimensionless $y$-velocity alongside the horizontal mid-span of the cubical cavity for $Ra = 10^5$ and $\phi = 0.03$ for three values of

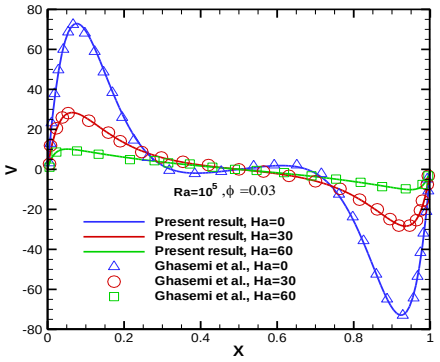


**Fig. 2** – Code validation with Ghasemi et al. [16]

Hartmann ($Ha = 0$, $Ha = 30$ and $Ha = 60$). Using the same correlations that Ghasemi et al. [16] used for calculating dynamic viscosity and thermal conductivity, it can be observed, that the current code results accord well with their results.

## 4. RESULTS AND DISCUSSION

This three-dimensional numerical study shed light on the free convection of $Fe_3O_4$-Water nanofluid inside a differentially heated cubic enclosure. Simulations are carried out for four Rayleigh numbers ($10^3, 10^4, 10^5$ and $10^6$), five values of solid volume frac-

tion of $Fe_3O_4$ in water base fluid ($\emptyset = 0, 0.01, 0.02, 0.03, 0.04$), five values of MF strength ($Ha = 0, 5, 10, 15, 20$) and three MF directions (Bx, By, Bz). Fig. 3(a) and 3(b) show the change in the $Nu_{avg}$ depending on $Ha$ (in each direction separately of the three principal directions of MF; *Bx*, *By* and *Bz*) for pure water ($\emptyset = 0$) and for 2% of solid volume fraction ($\emptyset = 0.02$) and this, for $Ra = 10^3$ and for $Ra = 10^6$ respectively. The first thing to notice is that an augment in concentration of $Fe_3O_4$ nnps leads to a higher heat exchange amount for the three directions of MF. Moreover, the reduction in heat exchange rate with the enhance in MF strength resulting from the development of Lorentz forces is evident for all MF directions. From these figures, it is also interesting to deduce, the prominent impact of changing the direction of MF on the thermal transfer rate in studied cavity. For $Ra = 10^3$, the greatest decrease in Nu is recorded when the MF is directed along the z axis and the smallest reduction is registered when the MF is directed in the y axis (see Fig. 3(a)). For $Ra = 10^6$, the greatest decrease in the thermal transfer is registered in the case where the MF is parallel to the temperature gradient, i.e. along directed along the *x* axis. In second position, it is the orientation of the magnetic field along the *z* axis which causes more reduction in the rate of heat transfer. When the MF is directed along the y axis, the smallest reduction in thermal transfer rate is recorded (see Fig. 3(b)).

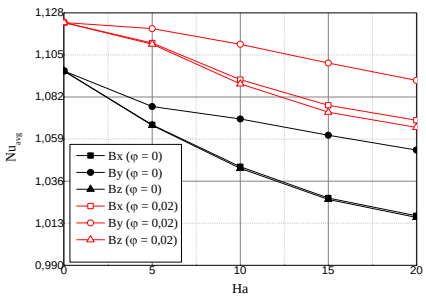


a)

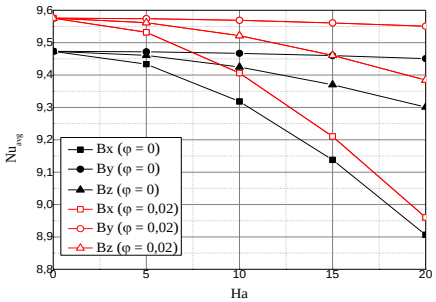


b)

**Fig. 3** – $Nu_{avg}$ at the hot wall with Ha for three MF directions. (a) $R_a = 10^3$ (b) $R_a = 10^6$

The same order in the MF directions for reducing the $Nu_{avg}$ was recorder for $Ra = 10^4$ and $Ra = 10^5$. Fig. 4(a) and 4(b) illustrate the impact of increasing the solid volume fraction of $Fe_3O_4$ in $H_2O$ and increasing the Ha number on the behavior of $Nu_{avg}$ at the hot wall, for two values of Ra: $Ra = 10^3$ and $Ra = 10^6$ when the MF is horizontally (*Bx*).

For all considered MF intensities, an increase of 1 % in the volume fraction of nnps leads to an increase of approximately 1.87 % in the Nu number for $Ra = 10^3$ and increase of 0.42 % in the Nu number for $Ra = 10^6$. Beyond $Ha = 5$, an increase of 5 in the intensity of MF (Ha) conducts to a reduction of approximately 0.91 % in the Nu number for $Ra = 10^3$ and a decrease of 0.1 % in the Nu number for $Ra = 10^6$. It is clear that the reduction of the thermal transfer rate is caused by the augment of Lorentz forces intensity resulting from MF application.

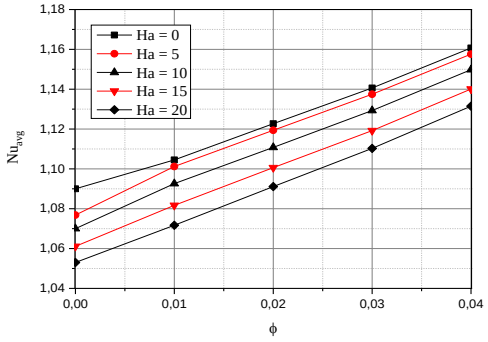


a)

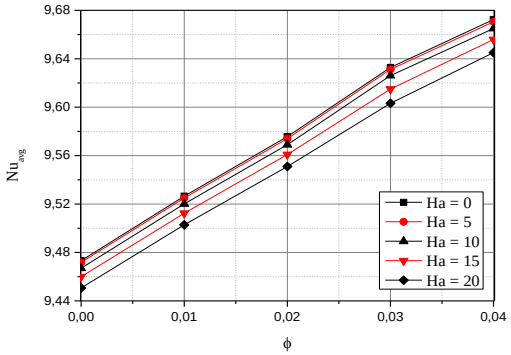


b)

**Fig. 4** – $Nu_{avg}$ at the hot wall with $\emptyset$ (*Bx*), (a) $R_a = 10^3$ and (b) $R_a = 10^6$

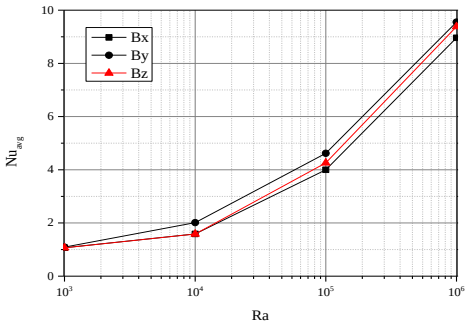


**Fig. 5** – $Nu_{avg}$ at hot wall with $R_a$ for $H_a = 20$, for three MF directions and for $\emptyset = 0.02$

The same phenomenon is observed when the MF is applied in the other two directions. Fig. 5 illustrates the impact of increasing $R_a$ on $Nu_{avg}$ at the hot wall for

one MF intensity ($Ha = 20$), for 2 % of solid volume fraction ($\emptyset = 0.02$), and for a MF applied each time in one of the principal directions.

It shows that with the increase in Ra number, the buoyancy forces are enhanced, thus strengthening the heat exchange inside the cubic cavity in the three directions. It can also be seen that when the magnetic field is parallel to the $x$-axis, the heat transfer rate is the weakest, which agrees with the above results. To investigate the impacts of buoyancy force on heat transfer in the cavity, Fig. 6 presents isotherms for a medium MF intensity ($Ha = 10$), applied along the $x$-axis and for 2 % of nnps volume fraction. It shows isotherms for the four Ra numbers considered in this study. The conduction regime dominates when the buoyancy force is weak $Ra = 10^3$. As the force gradually augments, the convective regime becomes large and dominant.

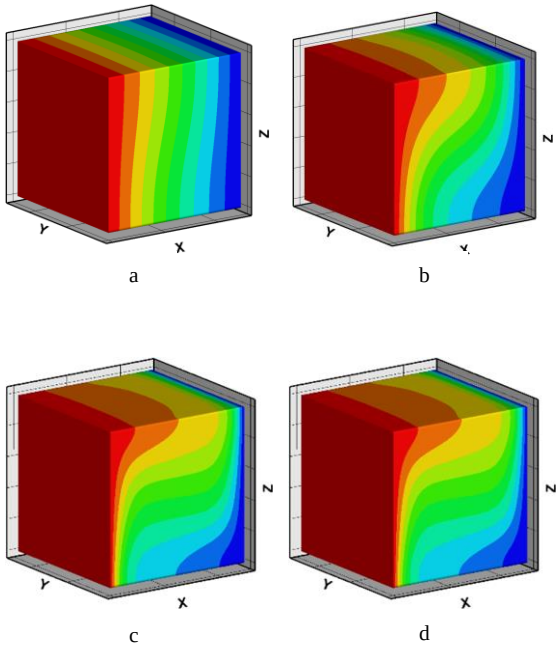


**Fig. 6** – Impact of Ra (a) $Ra = 10^3$, (b) $Ra = 10^4$, (c) $Ra = 10^5$, (d) $Ra = 10^6$ on isotherms for $Ha = 10$, $Bx$, $\emptyset = 0.02$ $Ra = 10^3$ and a reduction of 0.1 % in the Nu number for $Ra = 10^6$

The dominance of the conductive regime because of the feebleness of the buoyancy force is confirmed by the parallelism of the isotherms with differentially heated walls ($Ra = 10^3$). As the intensity of the buoyancy force increases by rising Ra, the convection becomes strong and dominates ($Ra = 10^6$). Both isotherms and streamlines are presented in Fig. 7 (a), (b) and (c) at the enclosure middle plane ($Y = 0.5$) to see the effects of the increase in the intensity of a horizontal MF ($H_a = 0$, $H_a = 5$ and $H_a = 20$ respectively) on the behavior of the flow inside the cavity for $\emptyset = 0.03$ and $Ra = 10^4$. Due to the weak buoyancy force, the streamlines represent one main vortex. As Lorentz forces increases, the principal vortex rotates reverse. Initially, oval becomes more circular, the flow is slowed down, hence the explanation of decreasing the thermal transfer rate. To examine the impact of MF direction, isotherms and streamlines at the same middle plane are presented for $H_a = 20$, $Ra = 10^6$, and for nnps volume fraction of 4% on Fig. 7 (d), (e) and (f).

Since for this Rayleigh value, the buoyancy force is strong, the principal vortex caused by the movement of six selected particles are stronger. It is evident that there are two eddies within the vortex formed by the movement of these six particles. The existence of to such vortexes causes he appearance of a strong thermal plume and makes the isotherms denser near the hot wall. The movement of particles becomes uniform when the MF is applied in the $x$-direction, which means that applying MF in this direction diminishes the thermal transfer rate greater than in the $y$ and $z$ directions.

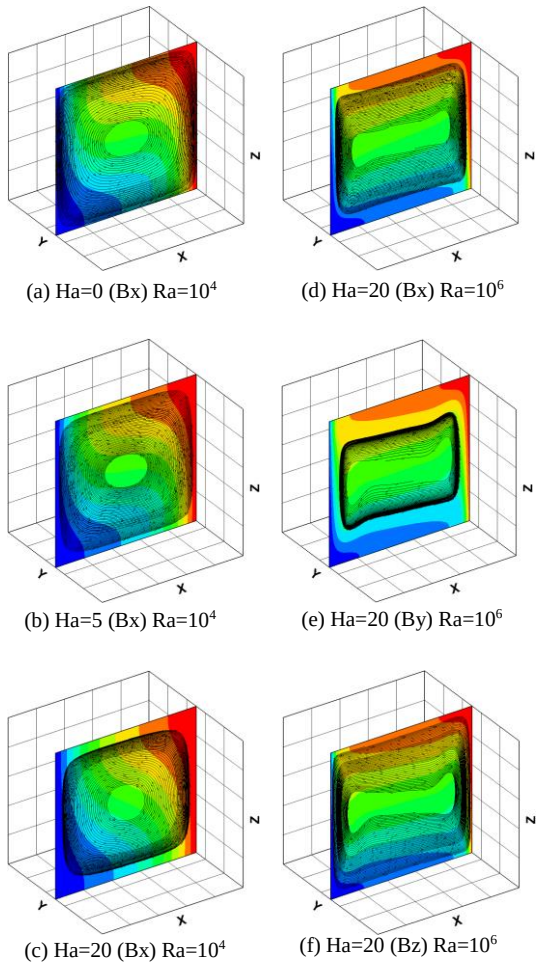


**Fig. 7** – Effects of $H_a$ (a) $H_a$ = 0, (b) $H_a$ = 5, (c) $H_a$ = 20 on streamlines and isotherms for $Ra = 10^4$, $Bx$ and $\emptyset = 0.03$ and effects of MF directions (d) $Bx$, (e) $By$, (f) $Bz$ on streamlines and isotherms for $H_a = 20$, $Ra = 10^6$ and $\emptyset = 0.04$

## 5. CONCLUSION

This 3D numerical simulation aims to highlight how changing the direction of a uniform magnetic field applied from outside affects the convection of $Fe_3O_4$-water nanofluid filling a cubic container. The results indicate that MF can control natural convection in a cubical cavity. The free convection in the enclosure is enhanced with the intensification of the buoyancy forces and also, with the rise in the solid volume fraction. On the other

hand, the rise in the intensity of the Lorentz force resulting from the application of a uniform external MF in one of the three main directions suppresses the free convection in the nanofluid. For all considered MF intensities, an increase of 1 % in the volume fraction of nnps leads to an increase of 1.87 % in the Nu number for $Ra = 10^3$ and increase of 0.42 % in the Nu number for $Ra = 10^6$. Beyond $Ha = 5$, an increase of 5 in the intensity of MF (Ha) conducts to a reduction of 0.91 % in the Nu number for As the MF magnitude increases, the decrease slope of Nusselt number augments with the increasing of Rayleigh number. With conduction dominance $Ra = 10^3$, the greatest damping of the heat exchange rate is recorded when the MF is directed horizontally in x direction and the smallest reduction is registered when the MF is along the y axis. With convective regime dominance ($Ra = 10^4, 10^5$ *and* $10^6$), applying the MF parallel to the temperature gradient reduces convection more than the other two directions. In the second position, it is the orientation of the MF according to the gravitational direction (vertical direction) which further reduces the rate of convective exchange in the cavity.

## NOMENCLATURE

| SYMBOL | DESCRIPTION |
|---|---|
| $\boldsymbol{B_0}$ | Magnetic field (MF) [Tesla] |
| $\vec{\boldsymbol{B}}$ | Dimensionless MF density vector |
| $\boldsymbol{C_p}$ | Specific heat [J/(kg·K)] |
| $\vec{\boldsymbol{e_B}}$ | Unitary vector of the direction of $\vec{B}$ |
| $g$ | Gravitational acceleration [m/s$^2$] |
| $Ha$ | Hartmann number |
| $J$ | Electrical current density [A/m] |
| $k$ | Thermal conductivity, [W/(m·K)] |
| $L$ | Cubical cavity side [m] |
| Nu | Local Nusselt number |
| $P$ | Dimensionless pressure |
| $Pr$ | Prandtl number |
| $R_a$ | Rayleigh number |
| $T$ | Temperature [K] |
| $U, V, W$ | Dimensionless velocity components |
| $\vec{\boldsymbol{V}}$ | Dimensionless velocity vector |
| $x, y, z$ | Cartesian coordinates [m] |
| $X, Y, Z$ | Dimensionless coordinates |
| **GREEK SYMBOLS** | |
| $\boldsymbol{\alpha}$ | Thermal diffusivity [m$^2$/s] |
| $\boldsymbol{\beta}$ | Thermal expansion coefficient, [1/K] |
| $\boldsymbol{\Phi}$ | Electrical potential [V] |
| $\boldsymbol{\phi}$ | Solid volume fraction |
| μ | Dynamic viscosity [kg /(m·s)] |
| $\boldsymbol{\nu}$ | Kinematic viscosity [m$^2$/s] |
| $\boldsymbol{\theta}$ | Dimensionless temperature $(T - T_c)/(T_h - T_c)$ |
| $\boldsymbol{\rho}$ | Density [kg/m$^3$] |
| $\boldsymbol{\sigma}$ | Electrical conductivity, μ$S$ cm$^{-1}$ |
| **SUBSCRIPTS** | |
| $Avg$ | Average |
| $c$ | Cold |
| $h$ | Hot |
| $f$ | Base-fluid |
| $nf$ | Nanofluid |
| $s$ | Nanoparticle |
| $x, y, z$ | Directions |

## REFERENCES


1. S.U.S. Choi, J.A. Eastman, *ASME International Mechanical Engineering Congress & Exposition*, San Francisco, CA, November 12 (1995).
2. D. Dey, D.S. Sahu, *HEAT TRANSFER Asian Research* 1 (2020)
3. M. Hajiyan, S. Mahmud, M. Biglarbegian, H.A. Abdullah, A. Chamkha, *International Journal of Numerical Methods for Heat & Fluid Flow* **29** No 4, 1466 (2018).
4. Z. Boulahia, C. Boulahia, R. Sehaqui, *Arabian Journal for Science and Engineering* **46**, 2985 (2021).
5. L. El Moutaouakil, M. Boukendil, Z. Zrikem, A. Abdelbaki, *International Journal of Heat and Technology* **38** No 1, 59 (2020).
6. M. Ferhi, R. Djebali, W. Al-Kouz, S. Abboudi, A.J. Chamkha, *Heat Transfer Asian Research* 1 (2020).
7. O. Giwa, M. Sharifpur, M.H. Ahmadi, J.P. Meyer, *Journal of Thermal Analysis and Calorimetry* (2020).
8. C.J. Ho, M.W. Chen, Z.W. Li, *International Journal of Heat and Mass Transfer* **51**, 4506 (2008)
9. D. Toghraie, S.M. Alempour, M. Afrand, *Journal of Magnetism and Magnetic Materials* **417**, 243 (2016).
10. M. Afrand, D. Toghraie, N. Sina, *International Communications in Heat and Mass Transfer* **75**, 262 (2016).
11. M. Sheikholeslami, R. Ellahi, K. Vafai, *Alexandria Engineering Journal* **57**, 565 (2018).
12. K. Khanafaer, K. Vafai, M. Lightstone, *International Journal of Heat and Mass Transfer* **46**, 5181 (2003).
13. H.F. Oztop, E. Abu-Nada, *International Journal of Heat and Fluid Flow* **29**, 1326 (2008).
14. J.C. Maxwell, *Oxford University Press* (Cambridge: 1904).
15. S.V. Patankar, *Numerical Heat Transfer and Fluid Flow, Hemisphere* (McGraw Hill, New York: 1980).
16. B. Ghasemi, S.M. Aminossadati, A. Raisi, *International Journal of Thermal Sciences* **50**, 1748 (2011).

# Природна MHD конвекція нанофлюїду $Fe_3O_4$-вода в кубічній порожнині

M. Maache Battira[1], C. Brahmi[1], R. Bessaih[2]

[1] *Abbes Laghrour University, Faculty of Science and Technology, Department of Mechanical Engineering, 40000 Khenchela, Algeria*
[2] *Mentouri University, Faculty of Science and Technology, Department of Mechanical Engineering, 25000 Constantine, Algeria*

Чисельно досліджено вплив трьох основних напрямків однорідного зовнішнього магнітного поля на вільну конвекцію в диференційовано нагрітій і заповненій нанофлюїдом $Fe_3O_4$-$H_2O$ кубічної порожнини. Для дискретизації системи диференціальних рівнянь у частинних похідних, що керують МГД-явищем, обрано метод скінченного об'єму, а числову роздільну здатність виконано за допомогою програмного забезпечення Ansys-Fluent 14.5. У цій роботі задачу досліджували для чистої води (∅=0), потім для води з додаванням малих часток наночастинок (∅=1%, 2%, 3% і 4%). Вплив трьох основних напрямків магнітного поля, числа Гартмана ($Ha = 0, 5, 10, 15$ і $20$)) і числа Релея ($Ra = 10^3$, $10^4$, $10^5$ і $10^6$), на термогідродинамічну поведінку нанофлюїдів. Теплопровідність і динамічна в'язкість визначаються кореляціями, спеціально розробленими для нанофлюїду $Fe_3O_4$-$H_2O$ з попередніх експериментальних робіт. Результати цього чисельного моделювання показують, що чим більше збільшується значення числа Релея, тим сильнішим стає нахил зменшення числа Нуссельта зі збільшенням інтенсивності магнітного поля. Горизонтальне застосування магнітного поля, тобто паралельне градієнту температури, зменшує передачу тепла більше, ніж два інших напрямки. У другому положенні найбільше зменшення швидкості конвективного теплообміну фіксується при вертикальному напрямку магнітного поля, тобто в напрямку сили тяжіння.

**Ключові слова:** Кубічна порожнина, Природна конвекція, Напрямок магнітного поля, Нанофлюїд $Fe_3O_4$-$H_2O$.